

# Agree to Disagree: Diversity through Disagreement for Better Transferability

Matteo Pagliardini<sup>1</sup> Martin Jaggi<sup>1</sup> François Fleuret<sup>1</sup> Sai Praneeth Karimireddy<sup>1,2</sup>

## Abstract

Gradient-based learning algorithms have an implicit *simplicity bias* which in effect can limit the diversity of predictors being sampled by the learning procedure. This behavior can hinder the transferability of trained models by (i) favoring the learning of simpler but spurious features — present in the training data but absent from the test data — and (ii) by only leveraging a small subset of predictive features. Such an effect is especially magnified when the test distribution does not exactly match the train distribution—referred to as the Out of Distribution (OOD) generalization problem. However, given only the training data, it is not always possible to apriori assess if a given feature is spurious or transferable.

Instead, we advocate for learning an ensemble of models which capture a diverse set of predictive features. Towards this, we propose a new algorithm D-BAT (Diversity-By-disAgreement Training), which enforces agreement among the models on the training data, but disagreement on the OOD data. We show how D-BAT naturally emerges from the notion of generalized discrepancy, as well as demonstrate in multiple experiments how the proposed method can mitigate shortcut-learning, enhance uncertainty and OOD detection, as well as improve transferability.

## 1. Introduction

While gradient-based learning algorithms such as Stochastic Gradient Descent (SGD), are nowadays ubiquitous in the training of Deep Neural Networks (DNNs), it is well known that the resulting models are (i) brittle when exposed to small distribution shifts (Beery et al., 2018; Sun et al., 2016; Amodei et al., 2016), (ii) can easily be fooled by small adversarial perturbations (Szegedy et al., 2014), (iii) tend to pick up spurious correlations (McCoy et al., 2019; Oaken-Rayner et al., 2020; Geirhos et al., 2020) — present in

the training data but absent from the downstream task —, as well as (iv) fail to provide adequate uncertainty estimates (Kim et al., 2016; van Amersfoort et al., 2020; Liu et al., 2021). Recently those learning algorithms have been investigated for their implicit bias toward simplicity — known as Simplicity Bias (SB), seen as one of the reasons behind their superior generalization properties (Arpit et al., 2017; Dziugaite & Roy, 2017). While for deep neural networks, simpler decision boundaries are often seen as less likely to overfit, Shah et al., 2020 demonstrated that the SB can still cause the aforementioned issues. In particular, they show how the SB can be *extreme*, compelling predictors to rely only on the simplest feature available, despite the presence of equally or even more predictive complex features.

Its effect is greatly increased when we consider the more realistic out of distribution (OOD) setting (Ben-Tal et al., 2009), in which the source and target distributions are different, known to be a challenging problem (Sagawa et al., 2020; Krueger et al., 2021). The difference between the two domains can be categorized into either a distribution shift — e.g. a lack of samples in certain parts of the data manifold due to limitations of the data collection pipeline —, or as simply having completely different distributions. In the first case, the SB in its extreme form would increase the chances of learning to rely on spurious features — shortcuts not generalizing to the target distribution. Classic manifestations of this in vision applications are when models learn to rely mostly on textures or backgrounds instead of more complex and likely more generalizable semantic features such as using shapes (Beery et al., 2018; Ilyas et al., 2019; Geirhos et al., 2020). In the second instance, by relying only on the simplest feature, and being invariant to more complex ones, the SB would cause confident predictions (low uncertainty) on completely OOD samples. This even if complex features are contradicting simpler ones. Which brings us to our goal of deriving a method which can (i) learn more transferable features, better suited to generalize despite distribution shifts, and (ii) provides accurate uncertainty estimates also for OOD samples.

We aim to achieve those two objectives through learning an ensemble of diverse predictors  $(h_1, \dots, h_K)$ , with  $h : \mathcal{X} \rightarrow \mathcal{Y}$ , and  $K$  being the ensemble size. Suppose that our training data is drawn from the distribution  $\mathcal{D}$ , and  $\mathcal{D}_{\text{ood}}$  is the distribution of OOD data on which we will be tested.

<sup>1</sup>EPFL <sup>2</sup>UC Berkeley. Correspondence to: Matteo Pagliardini <matteo.pagliardini@epfl.ch>.

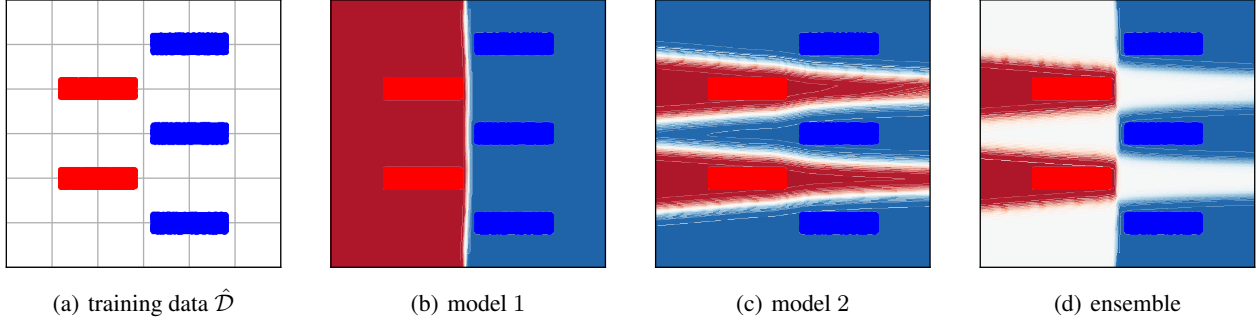


Figure 1. Example of applying D-BAT on a simple 2D toy example similar to the LMS-5 dataset introduced by Shah et al. (2020). The two classes, red and blue, can easily be separated by a vertical boundary decision. Other ways to separate the two classes — with horizontal lines for instance — are more complex, i.e. they require more hyperplanes. The simplicity bias will push models to systematically learn the simpler feature, as in the second column (b). Using D-BAT, we are able to learn the model in column (c), relying on a more complex boundary decision, effectively overcoming the simplicity bias. The ensemble  $h_{ens}(x) = h_1(x) + h_2(x)$ , in column (d), outputs a flat distribution at points where the two models disagree, effectively maximizing the uncertainty at those points. In this experiments the samples from  $\mathcal{D}_{ood}$  were obtained through computing adversarial perturbations, see App. C.2 for more details.

Importantly,  $\mathcal{D}$  and  $\mathcal{D}_{ood}$  may have non-overlapping support, and  $\mathcal{D}_{ood}$  is not known during training. Our proposed method, D-BAT (Diversity-By-disAgreement Training), relies on the following idea:

*Diverse hypothesis should agree on the source distribution  $\mathcal{D}$  while disagreeing on the OOD distribution  $\mathcal{D}_{ood}$ .*

Intuitively, a set of hypotheses should agree on what is known i.e. on  $\mathcal{D}$ , while formulating different interpretations of what is *not* known, i.e. on  $\mathcal{D}_{ood}$ . Even if each *individual predictor* might be wrongly confident on OOD samples, while predicting different outcomes — the resulting uncertainty of the *ensemble* on those samples will be increased. Disagreement on  $\mathcal{D}_{ood}$  can itself be enough to promote learning diverse representations of instances of  $\mathcal{D}$ . In the context of object detection, if one model  $h_1$  is relying on textures only, this model will generate predictions on  $\mathcal{D}_{ood}$  based on textures, when enforcing disagreement on  $\mathcal{D}_{ood}$ , a second model  $h_2$  would be discouraged to use textures in order to disagree with  $h_1$  — and consequently look for a different hypothesis to classify instances of  $\mathcal{D}$  e.g. using shapes. This process is illustrated in Fig. 2. A 2D direct application of our algorithm can be seen in Fig. 1. Once trained, the ensemble can either be used by forming a weighted average of the probability distribution from each hypothesis, or by tuning the weights on a downstream task.

**Contributions.** Our results can be summarized as:

- We introduce D-BAT, a simple yet efficient novel diversity-inducing regularizer which enables training ensembles of diverse predictors.
- We provide a proof, in a simplified setting, that D-BAT promotes diversity, encouraging the models to utilize different predictive features.

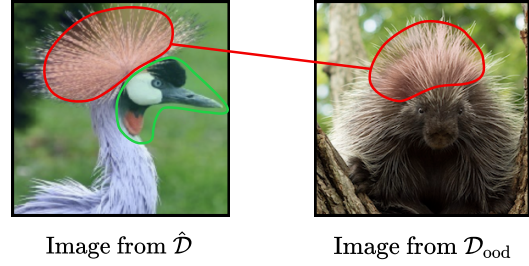


Figure 2. Illustration of how D-BAT can promote learning diverse features. Consider the task of classifying bird pictures among several classes. The red color represents the attention of a first model  $h_1$ . This model learnt to use some simple yet discriminative feature to recognise an African Crowned Crane on the left. Now suppose we use the right image  $\mathcal{D}_{ood}$  on which the models must disagree.  $h_2$  cannot again use the same feature as  $h_1$  since then it will not disagree on  $\mathcal{D}_{ood}$ . Instead,  $h_2$  would look for other distinctive features of the crane which are not present on the right e.g. using its beak and red throat pouch.

- We show on several datasets of varying complexity how the induced diversity can help to (i) tackle shortcut learning, and (ii) improve uncertainty estimation and transferability.

## 2. Related Work

**Diversity in ensembles.** It is intuitive that in order to gain from ensembling several predictors  $h_1, \dots, h_K$ , those should be diverse. The bias-variance-covariance decomposition (Ueda & Nakano, 1996), which generalizes the bias variance decomposition to ensembles, shows how the error decreases with the covariance of the members of the ensemble. Despite its importance, there is still no well accepted definition and understanding of diversity, and it is often derived from prediction errors of members of the ensemble (Zhou, 2012).

This creates a conflict between trying to increase accuracy of individual predictors  $h$ , and trying to increase diversity. In this view, creating a good ensemble is seen as striking a good balance between individual performance and diversity. To promote diversity in ensembles, a classic approach is to add stochasticity into the training by using different subsets of the training data for each predictor (Breiman, 1996), or using different data augmentation methods (Stickland & Murray, 2020). Another approach is to add orthogonality constraints on the predictor’s gradient (Ross et al., 2020; Kariyappa & Qureshi, 2019). Recently, the information bottleneck (Tishby et al., 2000) has been used to promote ensemble diversity (Ramé & Cord, 2021; Sinha et al., 2021). Unlike the aforementioned methods, D-BAT can be trained on the full dataset, it importantly does not set constraints the output of in-distribution samples, but on a separate OOD distribution. Furthermore, as opposed to Sinha et al. (2021), our individual predictors do not share the same encoder.

**Simplicity bias.** While the simplicity bias, by promoting simpler decision boundary, can act as an implicit regularizer and improves generalization (Arpit et al., 2017; Gunasekar et al., 2018), it is also contributing to the brittleness of gradient-based machine-learning (Shah et al., 2020). Recently Teney et al. (2021) proposed to evade the simplicity bias by adding gradient orthogonality constraints, not at the output level, but at an intermediary hidden representation obtained after a shared and fixed encoder. While their results are promising, the reliance on a pre-trained encoder limits the type of features that can be used to the set of features extracted by the encoder, especially, if a feature was already discarded by the encoder due to SB, it is effectively lost. In contrast, our method is not relying on a pre-trained encoder, also comparatively require a very small ensemble size to counter the simplicity bias.

**Shortcut learning.** The failures of DNNs across application domains due to shortcut learning have been documented extensively in (Geirhos et al., 2020). They introduce a taxonomy of predictors distinguishing between (i) predictors which can be learnt from the training algorithms (ii) predictors performing well on in-distribution training data, (iii) predictors performing well on in-distribution test data, and finally (iv) predictors performing well on in-distribution and OOD test data. The last category being the intended solutions. In our experiments, by learning diverse predictors, D-BAT increases the chance of finding one solution generalizing to both in and out of distribution test data, see § 4.1 for more details.

**OOD generalization.** Generalizing to distributions not seen during training is accomplished by two approaches: robust training, and invariant learning. In the former, the test distribution is assumed to be within a set of known plausible distributions (say  $\mathcal{U}$ ). Then, robust training minimizes the

loss over the worst possible distribution in  $\mathcal{U}$  (Ben-Tal et al., 2009). Numerous approaches exist to defining the set  $\mathcal{U}$  - see survey by (Rahimian & Mehrotra, 2019). Most recently, Sagawa et al. (2020) model the set of plausible domains as the convex hull over predefined subgroups of datapoints and Krueger et al. (2021) extend this by taking affine combinations beyond the convex hull. Our approach also borrows from this philosophy - when we do not know the labels of the OOD data, we assume the worst case and try predict as diverse labels as possible. This is similar to the notion of discrepancy introduced in domain adaptation theory (Mansour et al., 2009; Cortes & Mohri, 2011; Cortes et al., 2019). A different line of work defines a set of environments and asks that our outputs be ‘invariant’ (i.e. indistinguishable) among the different environments (Bengio et al., 2013; Arjovsky et al., 2019; Koyama & Yamaguchi, 2020). When only a single training environment is present, like in our setting, this is akin to adversarial domain adaptation. Here, the data of one domain is modified to be indistinguishable to the other (Ganin et al., 2016; Long et al., 2017). However, this approach is fundamentally limited. E.g. in Fig. 2 a model which classifies both the crane and the porcupine as a crane is invariant, but incorrect.

**Uncertainty estimation.** DNNs are notoriously unable to provide reliable confidence estimates, which is impeding the progress of the field in safety critical domains (Begoli et al., 2019), as well as hurting models interpretability (Kim et al., 2016). To improve the confidence estimates of DNNs, Gal & Ghahramani (2016) propose to use dropout at inference time, a method referred to as MC-Dropout. Other popular methods used for uncertainty estimation are Bayesian Neural Networks (BNNs) (Hernández-Lobato & Adams, 2015) and Gaussian Processes (Rasmussen & Williams, 2005). All those methods but gaussian processes, were recently shown to fail to adequately provide high uncertainty estimates on OOD samples *away* from the boundary decision (van Amersfoort et al., 2020; Liu et al., 2021). We show in our experiments how D-BAT can help to associate high uncertainty to those samples by maximizing the disagreement outside of  $\mathcal{D}$  (see § 4.3, as well as Fig.1).

## 3. Diversity through Disagreement

### 3.1. Motivating D-BAT

We will first define some notation and explain why standard training fails for OOD generalization. Then, we introduce the concept of discrepancy which will motivate our D-BAT algorithm.

**Setup.** Let us formally define the OOD problem.  $\mathcal{X}$  is the input space,  $\mathcal{Y}$  the output space, we define a domain as a pair of a distribution over  $\mathcal{X}$  and a labeling function  $h : \mathcal{X} \rightarrow \mathcal{Y}$ . Given any distribution  $\mathcal{D}$  over  $\mathcal{X}$ , given

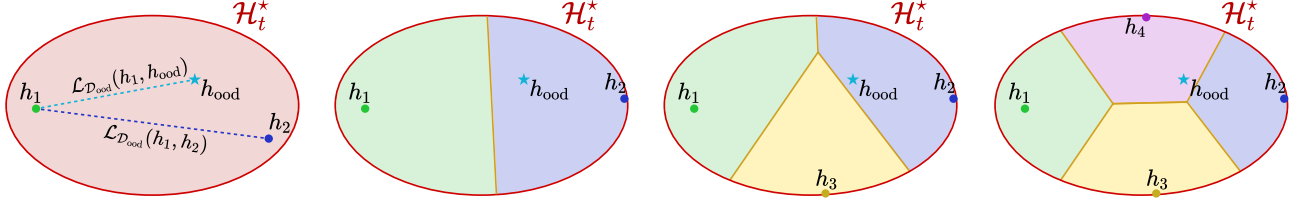


Figure 3. If  $h_1$  is computed by minimizing the training loss on  $\mathcal{D}$ , its loss on the OOD task  $\mathcal{D}_{\text{ood}}$  may be very large i.e.  $h_1$  may be very far from the optimal OOD model  $h_{\text{ood}}$  as measured by  $\mathcal{L}_{\mathcal{D}_{\text{ood}}}(h_1, h_{\text{ood}})$  (left). To mitigate this, we propose to learn a diverse ensemble  $\{h_1, \dots, h_4\}$  which is maximally ‘spread-out’ (with distance measured using  $\mathcal{L}_{\mathcal{D}_{\text{ood}}}(\cdot, \cdot)$ ) and cover the entire space of possible solutions  $\mathcal{H}_t^*$ . This minimizes the distance between the unknown  $h_{\text{ood}}$  and our learned ensemble, ensuring we learn transferable features with good performance on  $\mathcal{D}_{\text{ood}}$ .

two labeling functions  $h_1$  and  $h_2$ , given a loss function  $L : \mathcal{Y} \times \mathcal{Y} \rightarrow \mathbb{R}_+$ , we define the expected loss as the expectation:  $\mathcal{L}_{\mathcal{D}}(h_1, h_2) = \mathbb{E}_{x \sim \mathcal{D}}[L(h_1(x), h_2(x))]$ .

Now, suppose that the training data is drawn from the distribution  $(\mathcal{D}_t, h_t)$ , but we will be tested on a different distribution  $(\mathcal{D}_{\text{ood}}, h_{\text{ood}})$ . While the labelling function  $h_{\text{ood}}$  is unknown, we assume that we have access to unlabelled samples from  $\mathcal{D}_{\text{ood}}$ .

Finally, let  $\mathcal{H}$  be the set of all labelling functions i.e. the set of all possible prediction models. And further define  $\mathcal{H}_t^*$  and  $\mathcal{H}_{\text{ood}}^*$  to be the optimal labelling functions on the train and the OOD domains:

$$\mathcal{H}_t^* := \arg \min_{h \in \mathcal{H}} \mathcal{L}_{\mathcal{D}_t}(h, h_t), \quad \mathcal{H}_{\text{ood}}^* := \arg \min_{h \in \mathcal{H}} \mathcal{L}_{\mathcal{D}_{\text{ood}}}(h, h_{\text{ood}}).$$

We assume that there exists an ideal transferable function  $h^* \in \mathcal{H}_t^* \cap \mathcal{H}_{\text{ood}}^*$ . This assumption captures the reality that the training task and the OOD testing task are closely related to each other. Otherwise, we would not expect any OOD generalization.

**Beyond standard training.** Just using the training data, standard training would train a model  $h_{\text{ERM}} \in \mathcal{H}_t^*$ . However, as we discussed in the introduction, if we use gradient descent to find the ERM solution, then  $h_{\text{ERM}}$  will likely be the simplest model i.e. it will likely pick up spurious correlations in  $\mathcal{D}_t$  which are not present in  $\mathcal{D}_{\text{ood}}$ . Thus, the error on OOD data might be very high

$$\mathcal{L}_{\mathcal{D}_{\text{ood}}}(h_{\text{ERM}}, h_{\text{ood}}) \leq \max_{h \in \mathcal{H}_t^*} \mathcal{L}_{\mathcal{D}_{\text{ood}}}(h, h_{\text{ood}}).$$

Instead, we would ideally like to *minimize* the right hand side in order to find  $h^*$ . The main difficulty is of course that we do not have access to the OOD labels  $h_{\text{ood}}$ . So we can instead use the following proxy:

$$\mathcal{L}_{\mathcal{D}_{\text{ood}}}(h_1, h_{\text{ood}}) \leq \max_{h_2 \in \mathcal{H}_t^*} \mathcal{L}_{\mathcal{D}_{\text{ood}}}(h_1, h_2)$$

In the above we used the fact that  $\mathcal{H}_t^* \cap \mathcal{H}_{\text{ood}}^*$  is non-empty. Recall that  $\mathcal{H}_t^* = \arg \min_{h \in \mathcal{H}} \mathcal{L}_{\mathcal{D}_t}(h, h_t)$ . So this means

we want to pick  $h_2$  to minimize our training data (i.e. belong to  $\mathcal{H}_t^*$ ), but otherwise maximally disagree with  $h_1$  on the OOD data — this process is illustrated in Fig. 3. The latter is closely related to the concept of discrepancy in domain-adaptation (Mansour et al., 2009; Cortes et al., 2019). However, the main difference between the definitions is that we restrict the maximum to the set of  $\mathcal{H}_t^*$ , whereas the standard notions use an unrestricted maximum. Thus, our version is tighter when the train and OOD tasks are closely related.

**Deriving D-BAT.** We make two final changes to the discrepancy term above to derive D-BAT. First, if  $\mathcal{L}_{\mathcal{D}}(h_1, h_2)$  is a loss function which quantifies dis-agreement, then suppose we have another loss function  $\mathcal{A}_{\mathcal{D}}(h_1, h_2)$  which quantifies agreement. Then, we can minimize agreement instead of maximizing dis-agreement

$$\arg \min_{h_2 \in \mathcal{H}_t^*} \mathcal{A}_{\mathcal{D}}(h_1, h_2) = \arg \max_{h_2 \in \mathcal{H}_t^*} \mathcal{L}_{\mathcal{D}}(h_1, h_2).$$

Secondly, we relax the constrained formulation  $h_2 \in \mathcal{H}_t^*$  by adding a penalty term with weight  $\alpha$  as

$$h_{\text{D-BAT}} \in \min_{h_2 \in \mathcal{H}} \underbrace{\mathcal{L}_{\mathcal{D}_t}(h_2, h_t)}_{\text{fit train data}} + \alpha \underbrace{\mathcal{A}_{\mathcal{D}_{\text{ood}}}(h_1, h_2)}_{\text{disagree on OOD}}.$$

The above is the core of our D-BAT procedure - given a first model  $h_1$ , we train a second model  $h_2$  to fit the training data  $\mathcal{D}$  while disagreeing from  $h_1$  on  $\mathcal{D}_{\text{ood}}$ . Thus, we have

$$\mathcal{L}_{\mathcal{D}_{\text{ood}}}(h_1, h_{\text{ood}}) \leq \max_{h_2 \in \mathcal{H}_t^*} \mathcal{L}_{\mathcal{D}_{\text{ood}}}(h_1, h_2) \approx \mathcal{L}_{\mathcal{D}_{\text{ood}}}(h_1, h_{\text{D-BAT}}),$$

implying that D-BAT gives us a good proxy for the unknown OOD loss, and can be used for uncertainty estimation. Following a similar argument for  $h_1$ , we arrive the following training procedure:

$$\min_{h_1, h_2} \frac{1}{2} (\mathcal{L}_{\mathcal{D}_t}(h_1, h_t) + \mathcal{L}_{\mathcal{D}_t}(h_2, h_t)) + \alpha \mathcal{A}_{\mathcal{D}_{\text{ood}}}(h_1, h_2).$$

However, we found the training dynamics for simultaneously learning  $h_1$  and  $h_2$  to be unstable. Hence, we propose a sequential variant which we describe next.



**Algorithm 1** D-BAT for binary classification

---

**Input:** train data  $\mathcal{D}$ , OOD data  $\mathcal{D}_{\text{ood}}$ , stopping time  $T$ , D-BAT coefficient  $\alpha$ , learning rate  $\eta$ , pre-trained model  $h_1$ , randomly initialized model  $h_2$  with weights  $\omega_0$ , and its loss  $\mathcal{L}$ .

**for**  $t \in 0, \dots, T-1$  **do**

**Sample**  $(x, y) \sim \mathcal{D}$

**Sample**  $\tilde{x} \sim \mathcal{D}_{\text{ood}}$

$\omega_{t+1} = \omega_t - \eta \nabla_{\omega} (\mathcal{L}(h_2, x, y) + \alpha \mathcal{A}(h_1, h_2, \tilde{x}))$

**end for**

---

### 3.2. Algorithm description

**Binary classification formulation.** Concretely given a binary classification task, with  $\mathcal{Y} = \{0, 1\}$ , we train two models sequentially. The training of the first model  $h_1$  is done in a classical way, minimizing its empirical classification loss  $\mathcal{L}(h_1(x), y)$  over samples  $(x, y)$  from  $\mathcal{D}$ .

$$h_1^* \in \operatorname{argmin}_{h_1 \in \mathcal{H}} \frac{1}{N} \sum_{(x, y) \in \mathcal{D}} \mathcal{L}(h_1(x), y)$$

Once  $h_1$  trained, we train the second model  $h_2$  adding a term  $\mathcal{A}_{\tilde{x}}(h_1, h_2)$  representing the agreement on samples  $\tilde{x}$  of  $\mathcal{D}_{\text{ood}}$ , with some weight  $\alpha \geq 0$ :

$$h_2^* \in \operatorname{argmin}_{h_2 \in \mathcal{H}} \frac{1}{N} \left( \sum_{(x, y) \in \mathcal{D}} \mathcal{L}(h_2(x), y) + \alpha \sum_{\tilde{x} \in \mathcal{D}_{\text{ood}}} \mathcal{A}_{\tilde{x}}(h_1, h_2) \right)$$

Given  $p_{h, \tilde{x}}^{(y)}$  the probability of class  $y$  predicted by  $h$  given  $\tilde{x}$ , the agreement  $\mathcal{A}_{\tilde{x}}(h_1, h_2)$  is defined as:

$$\mathcal{A}_{\tilde{x}}(h_1, h_2) = -\log(p_{h_1, \tilde{x}}^{(0)} \cdot p_{h_2, \tilde{x}}^{(1)} + p_{h_1, \tilde{x}}^{(1)} \cdot p_{h_2, \tilde{x}}^{(0)}) \quad (\text{AG})$$

In the case where  $\mathcal{L}$  is the binary cross-entropy loss, the composite  $\mathcal{L}_{\text{D-BAT}}$  training objective becomes:

$$\begin{aligned} \mathcal{L}_{\text{D-BAT}}(h_1, h_2, x, y, \tilde{x}) &= \mathcal{L}(h_2(x), y) + \alpha \mathcal{A}(h_1, h_2, \tilde{x}) \\ &= -\log(p_{h_2, x}^{(y)}) - \alpha \log(p_{h_1, \tilde{x}}^{(0)} \cdot p_{h_2, \tilde{x}}^{(1)} + p_{h_1, \tilde{x}}^{(1)} \cdot p_{h_2, \tilde{x}}^{(0)}) \end{aligned}$$

The algorithm for the binary classification formulation of D-BAT is straightforward and can be seen in Alg. 1.

**Multi-class classification formulation.** The previous formulation requires a distribution over two labels in order to compute the agreement term (AG). We extend the agreement term  $\mathcal{A}(h_1, h_2, \tilde{x})$  to the multi-class setting by binarizing the softmax distributions  $h_1(\tilde{x})$  and  $h_2(\tilde{x})$ . A simple way to do this is to take as positive class the predicted class of  $h_1$ :  $\tilde{y} = \operatorname{argmax}(h_1(\tilde{x}))$  with associated probability  $p_{h_1, \tilde{x}}^{(\tilde{y})}$ , while grouping the remaining complementary

**Algorithm 2** D-BAT for multi-class classification

---

**Input:** ensemble size  $M$ , train data  $\mathcal{D}$ , OOD data  $\mathcal{D}_{\text{ood}}$ , stopping time  $T$ , D-BAT coefficient  $\alpha$ , learning rate  $\eta$ , randomly initialized models  $(h_0, \dots, h_{M-1})$  with resp. weights  $(\omega_0^{(0)}, \dots, \omega_0^{(M-1)})$ , and a classification loss  $\mathcal{L}$ .

**for**  $m \in 0, \dots, M-1$  **do**

**for**  $t \in 0, \dots, T-1$  **do**

**Sample**  $(x, y) \sim \mathcal{D}$

**Sample**  $\tilde{x} \sim \mathcal{D}_{\text{ood}}$

$l_a \leftarrow 0$

$\tilde{y} \leftarrow \operatorname{argmax}_m h_m(\tilde{x})$

**for**  $i \in 0, \dots, m-1$  **do**

$l_a = l_a - \log(p_{h_i, \tilde{x}}^{(\tilde{y})} \cdot p_{h_m, \tilde{x}}^{(\neg \tilde{y})} + p_{h_i, \tilde{x}}^{(\neg \tilde{y})} \cdot p_{h_m, \tilde{x}}^{(\tilde{y})})$

**end for**

$\omega_{t+1}^{(m)} = \omega_t^{(m)} - \eta \nabla_{\omega^{(m)}} (\mathcal{L}(h_m, x, y) + \frac{\alpha}{M} l_a)$

**end for**

**end for**

---

class probabilities in a negative class  $\neg \tilde{y}$ . We would then have  $p_{h_1, \tilde{x}}^{(\neg \tilde{y})} = 1 - p_{h_1, \tilde{x}}^{(\tilde{y})}$ . We can then use the same bins to binarize the softmax distribution of the second model  $h_2(\tilde{x})$ . Another similarly sound approach would be to do the opposite and use the predicted class of  $h_2$  instead of  $h_1$ . In our experiments both approaches performed well. In Alg. 2 we show the second approach, which is a bit more computationally efficient in the case of ensembles of more than 2 predictors, as the binarization bins are built only once, instead of building them for each pair  $(h_i, h_m)$  for  $0 \leq i < m$ .

### 3.3. Learning diverse features

It is possible, under some simplifying assumptions to rigorously prove that minimizing  $\mathcal{L}_{\text{D-BAT}}$  results in learning predictors which use diverse features. We introduce the following theorem:

**Theorem 3.1** (D-BAT favors diversity). *Given a joint source distribution  $\mathcal{D}$  of triplets of random variables  $(C, S, Y)$  taking values in  $\{0, 1\}^3$ . Assuming  $\mathcal{D}$  has the following PMF:  $\mathbb{P}_{\mathcal{D}}(C = c, S = s, Y = y) = 1/2$  if  $c = s = y$ , and 0 otherwise, which intuitively corresponds to experiments § 4.1 in which two features (e.g. color and shape) are equally predictive of the label  $y$ . Assuming a first model learnt the posterior distribution  $\mathbb{P}_1(Y = 1 \mid C = c, S = s) = c$ , meaning that it is invariant to feature  $s$ . Given a distribution  $\mathcal{D}_{\text{ood}}$  uniform over  $\{0, 1\}^3$  outside of the support of  $\mathcal{D}$ , the posterior solving the D-BAT objective will be  $\mathbb{P}_2(Y = 1 \mid C = c, S = s) = s$ , invariant to feature  $c$ .*

The proof is provided in App. B. It crucially relies on the fact that  $\mathcal{D}_{\text{ood}}$  has positive weight on data points which only contain the alternative feature  $s$ , or only contain the feature  $c$ .

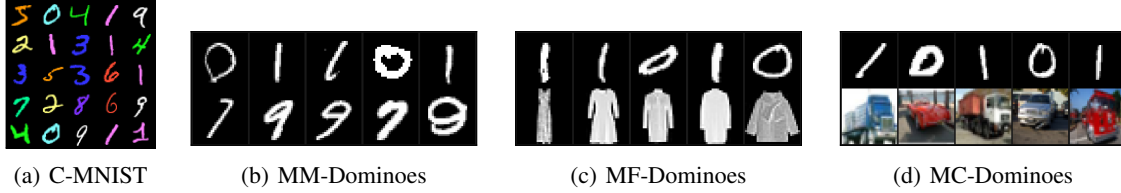


Figure 4. Samples from the training data distribution  $\mathcal{D}$  for C-MNIST, MM-Dominoes, MF-Dominoes, and MC-Dominoes. Those datasets are used to evaluate D-BAT’s aptitude to evade the simplicity bias. For C-MNIST, the simple feature is the color and the complex one is the shape. For all the Dominoes datasets, the simple feature is the top row, while the complex feature is the bottom one. One could indeed separate 0s from 1s by simply looking at the value of the middle pixels (if low value then 0 else 1).

Thus, as long as the  $\mathcal{D}_{\text{ood}}$  is supported on a diverse enough dataset with features present in different combinations (what we refer to as *counterfactual correlations*), we can expect D-BAT to learn models which utilize a variety of such features.

## 4. Experiments

We conduct three main types of experiments, (i) we evaluate how D-BAT can mitigate shortcut learning and effectively bypass the simplicity bias, (ii) we test the OOD detection capabilities of D-BAT models, (iii) finally we test the transferability of D-BAT learnt features.

### 4.1. Avoiding shortcuts

To know whether we learn a shortcut, and estimate our method’s ability to overcome the SB, we design five datasets of varying complexity with known shortcut in a similar fashion as Teney et al. (2021). Samples from those five datasets can be visualized in Fig. 4. For each dataset, we design various OOD distributions  $\mathcal{D}_{\text{ood}}$ . Samples from the different OOD distributions used can be visualized in App. D.

**Datasets.** We construct the following datasets.

- *C-MNIST*. The first dataset, which we name Colored-MNIST, or C-MNIST for short, consists of MNIST (Lecun & Cortes, 1998) images for which the color and the shape of the digits are equally predictive, i.e. all the 1 are pink, all the 5 are orange, etc. The color being simpler to learn than the shape, the simplicity bias will result in models trained on this dataset to rely solely on the color information while being invariant to the shape information. This dataset is a multiclass dataset with 10 classes.
- *C-MNIST—half*. This dataset is similar to the above C-MNIST dataset. The only difference being it is made only of the digits 0, 1, 2, 3, and 4. The remaining digits being used in  $\mathcal{D}_{\text{ood}}$  as clarified in § 4.1. This dataset is a multiclass dataset with 5 classes.
- *MM-Dominoes*. This binary classification dataset is made of concatenation of MNIST images. The first class is built concatenating images of 0s and 7s, while the second class is concatenating 1s and 9s. As it is easier to differentiate 0s vs 1s, the simplicity bias will compel models to only

rely on the first row, while being invariant to the second.

- *MF-Dominoes*. This binary classification dataset is made of concatenation of MNIST and Fashion-MNIST (Xiao et al., 2017) images. The first class is built concatenating images of 0s and images of coats, while the second class is concatenating 1s and images of dresses. As for the MM-Dominoes, it is easier to differentiate 0s vs 1s, the simplicity bias will therefore compel models to only rely on the first row, while being invariant to the second row.
- *MC-Dominoes*. This binary classification dataset is made of concatenation of MNIST images with CIFAR-10 (Krizhevsky, 2009) images. The first class is built concatenating images of 0s and images of cars, while the second class is concatenating 1s and images of trucks. Here again, trained model without D-BAT will be invariant to the second row. In this dataset the gap between the difficulty of the two rows is large. If images of 1s and 0s can be efficiently separated using a linear classifier with near perfect accuracy, the bottom row is (i) less predictive (cannot achieve 100% accuracy on its own) and (ii) requires more high level, non-linear features.

**$\mathcal{D}_{\text{ood}}$  used for the above datasets.** For the C-MNIST dataset, we use three different OOD distributions. The first one,  $\mathcal{D}_{\text{ood}}^{(1)}$  is made of random associations between colors and shapes, which includes 2% of in-distribution samples. The second one  $\mathcal{D}_{\text{ood}}^{(2)}$  is similar to the first one, except for the amount of in-distribution samples which is increased to 55%. The third distribution  $\mathcal{D}_{\text{ood}}^{(3)}$  follows the same principle with 82% in-distribution overlap. For the C-MNIST—half dataset, we only consider 2 OOD distributions.  $\mathcal{D}_{\text{ood}}^{(1)}$  is built using digits 5 to 9, not present in  $\mathcal{D}$ , combined with random colors similar to the ones in  $\mathcal{D}$ .  $\mathcal{D}_{\text{ood}}^{(2)}$  is also built using the same OOD digits but this time those are not combined with any color. For the three remaining Dominoes datasets, the OOD distributions are following the same principle.  $\mathcal{D}_{\text{ood}}^{(1)}$  is obtained by only combining images of 0s and 1s on the first row with on the second row the other class than the one used in  $\mathcal{D}$ , i.e. 0s with trucks instead of cars and 1s with cars instead of trucks.  $\mathcal{D}_{\text{ood}}^{(2)}$  is made of random associations between images of MNIST and resp. MNIST, Fashion-

Table 1. Results of our experiments on the five datasets described in § 4.1. We train several 2-model ensembles for each pair of  $(\mathcal{D}, \mathcal{D}_{\text{ood}})$ . The first column shows the accuracies (Acc) and randomized-accuracies with simplest feature randomized (R-Acc) for the first model trained in a standard way. We observe the R-Acc falls systematically to random guessing, despite a perfect Acc, indicating  $\mathcal{M}_1$  learnt to rely only on the simplest feature. The three remaining columns show the Acc and R-Acc for different  $\mathcal{D}_{\text{ood}}$  distributions, for the details of those distributions and a deeper analysis see § 4.1. We mark in bold the accuracy values close to random guessing.

Dataset $\mathcal{D}$	$\mathcal{M}_1$		$\mathcal{M}_2, \mathcal{D}_{\text{ood}}^{(1)}$		$\mathcal{M}_2, \mathcal{D}_{\text{ood}}^{(2)}$		$\mathcal{M}_2, \mathcal{D}_{\text{ood}}^{(3)}$	
	Acc	R-Acc	Acc	R-Acc	Acc	R-Acc	Acc	R-Acc
C-MNIST	100. $\pm$ 0.0	<b>12.3 <math>\pm</math> 0.7</b>	95.5 $\pm$ 0.7	90.2 $\pm$ 3.7	91.4 $\pm$ 1.7	45.7 $\pm$ 6.6	73.2 $\pm$ 7.7	31.3 $\pm$ 3.5
C-MNIST — half	100. $\pm$ 0.0	<b>27.1 <math>\pm</math> 2.8</b>	95.9 $\pm$ 0.4	90.1 $\pm$ 1.9	100. $\pm$ 0.0	<b>25.0 <math>\pm</math> 2.9</b>	-	-
M/M Dominoes	99.9 $\pm$ 0.0	<b>50.2 <math>\pm</math> 0.2</b>	99.9 $\pm$ 0.1	99.2 $\pm$ 0.1	98.5 $\pm$ 0.3	91.8 $\pm$ 1.3	98.9 $\pm$ 0.1	78.5 $\pm$ 3.2
M/F Dominoes	100. $\pm$ 0.0	<b>49.8 <math>\pm</math> 0.0</b>	98.1 $\pm$ 0.3	95.0 $\pm$ 0.3	97.1 $\pm$ 0.7	88.2 $\pm$ 0.6	95.4 $\pm$ 0.6	88.5 $\pm$ 0.4
M/C Dominoes	99.9 $\pm$ 0.0	<b>50.3 <math>\pm</math> 0.0</b>	96.2 $\pm$ 0.1	83.6 $\pm$ 1.4	92.8 $\pm$ 0.4	59.2 $\pm$ 1.1	90.4 $\pm$ 0.7	53.5 $\pm$ 0.9

MNIST, and CIFAR-10. Those include 2% in-distribution overlap. Finally,  $\mathcal{D}_{\text{ood}}^{(3)}$  is made by combining images of 0s and 1s with random OOD images of resp. MNIST, Fashion-MNIST, and CIFAR-10, *which are not* of classes used to build the training datasets.

**Experimental setup.** We use different variations of LeNet (Lecun et al., 1998) throughout all our experiments, see App. C.1. We use the AdamW optimizer (Loshchilov & Hutter, 2019) for all our experiments. For all the datasets in this section, we only train ensembles of 2 models, which we denote  $\mathcal{M}_1$  and  $\mathcal{M}_2$ . When building the OOD datasets, we make sure the images used are not shared with the images used to build the training, test and validation sets. To evaluate our method, we train D-BAT ensembles using several seeds for each  $(\mathcal{D}, \mathcal{D}_{\text{ood}})$  pair. We define the randomized-accuracy (R-Acc) as the accuracy over images where the simplest feature has been randomized. For the C-MNIST type of datasets, this means randomizing the color of digits, while for the dominoes datasets, this correspond to randomizing the first row (0s vs. 1s). We report averaged accuracies and randomized-accuracies in Tab. 1.

**Results and discussion.** First we look at results without D-BAT. Looking at the  $\mathcal{M}_1$  column in Tab. 1 we observe across datasets how all the accuracies are near 100% while the randomized-accuracies are near random guessing. This is a verification that without D-BAT, due to the simplicity bias, only the simplest feature is leveraged to predict the label and the models fail to generalize to domains for which the simple feature is spurious.

Next we examine results with D-BAT. When training the second model  $\mathcal{M}_2$  with D-BAT (see Tab. 1), we make several observations depending on the OOD distributions used. We learn that (i) given an OOD distribution with enough counterfactual correlations, D-BAT is effectively promoting models to use diverse features. This is demonstrated by the randomized accuracies of the second model being

Table 2. Transferability experiment: deep-ensembles and D-BAT models are trained on the Kaggle-Bird dataset (see § 4.2), and evaluated without fine-tuning on 44 overlapping classes of CUB-200. Results are averaged over 3 seeds.

method	accuracy	transfer accuracy
deep ensemble	96.9 $\pm$ 0.2	71.1 $\pm$ 0.6
D-BAT ( $\alpha = .001$ )	96.3 $\pm$ 0.2	73.9 $\pm$ 0.5

significantly higher than for the first model. We also observe (ii) that the model can tolerate overlaps between  $\mathcal{D}_{\text{ood}}$  and  $\mathcal{D}$ . We still get a randomized accuracy of 31.3% for the second model on C-MNIST despite a 82% in-distribution overlap. Finally, we see that (iii) when the weight on the counterfactual correlations is too small, it is harder to evade the simplicity bias. This is despite our theory predicting any non-zero weight is sufficient. This is likely because our theory was in the noise-free setting whereas real world datasets are noisy. We need at least enough weight to stand out from label noise.

## 4.2. Better Transferability

The experiments on shortcut learning in § 4.1 do provide a clear demonstration of how D-BAT can enhance the transferability of the learnt ensemble. Most of the ensembles in Tab. 1 can generalize to both domains where the simple feature is removed and where the complex feature is removed. In contrast, the baseline ensembles cannot generalize to domains where the simple feature is removed. In this section we provide additional results on a more challenging natural dataset where we do not know which features are spurious.

**Experimental setup.** For training, we use a 325 Bird Species dataset (Piosenka, 2020) found on kaggle which for simplicity we call the Kaggle-Bird dataset. This dataset shares 44 classes with the CUB-200 dataset (Welinder et al., 2010), which gives us a good framework to test how a

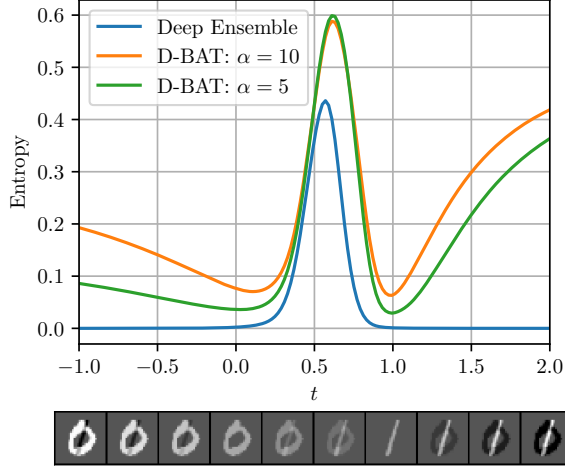


Figure 5. Entropy of ensembles of two models trained with and without D-BAT (deep-ensemble), for inputs  $x$  taken from along line  $t \cdot 1 + (1 - t) \cdot 0$  for  $t \in [-1, 2]$ . In-distribution samples are obtained for  $t \in \{0, 1\}$ . All ensembles have a similar test accuracy of 99%. Unlike deep ensembles, D-BAT ensembles are able to correctly give high uncertainty values for points far away from the decision boundary.

model can transfer from one to the other. For two methods, deep-ensembles and D-BAT, we train on Kaggle-Bird and measure the test accuracy on the Kaggle-Bird test set as well as the transfer accuracy obtained by using the pre-trained model on the 44 shared tasks — without fine-tuning. When training D-BAT, we use random crops of the MSCOCO (Lin et al., 2014) dataset as  $\mathcal{D}_{\text{ood}}$ . For mode details, see App. C.3.

**Results.** In Tab. 2 we observe (i) that both methods achieve comparable test accuracy on the Kaggle-Bird dataset, as well as (ii) that D-BAT transfers better to the shared CUB-200 classes. We also observed how our best D-BAT models were obtained with small  $\alpha$  values e.g.  $\alpha = 0.001$ . It is possible that larger values could further enhance the learnt representation, yet for those values, the ensemble might learn a shortcut, see § 5 for a more thorough discussion.

### 4.3. Better Uncertainty & OOD Detection

**MNIST setup.** We run two simple experiments to investigate D-BAT’s ability to provide good uncertainty estimates. The first one is similar to the MNIST experiment in Liu et al. (2021), it consists in learning to differentiate MNIST digits 0s from 1s. The uncertainty of the model — computed as the entropy — is then estimated for fake interpolated images of the form  $t \cdot 1 + (1 - t) \cdot 0$  for  $t \in [-1, 2]$ . An ideal model would assign (i) low uncertainty values for  $t$  near 0 and 1, corresponding to in-distribution samples, while (ii) high

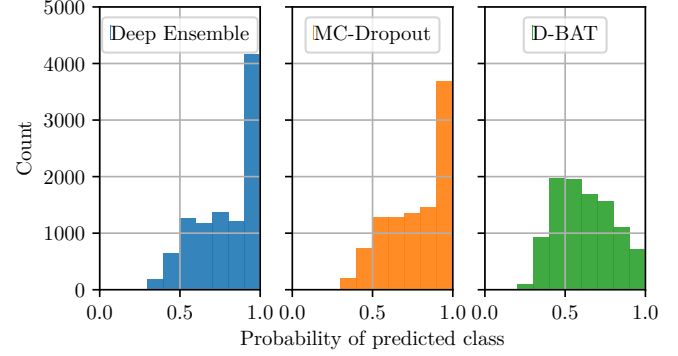


Figure 6. Histogram of predicted probabilities on OOD data. See § 4.3 for more details on the setup. D-BAT ensembles are better calibrated with less confidence on OOD data than deep-ensembles or MC-Dropout models.

uncertainty values elsewhere. In their experiments Liu et al. (2021) showed how only Gaussian Processes are able to fulfill those two conditions, most models failing in attributing high uncertainty *away* from the boundary decision (as it can also be seen in Fig. 1 when looking at individual models). We train ensembles of size 2 and average over 20 seeds. For D-BAT, we use as  $\mathcal{D}_{\text{ood}}$  the remaining (OOD) digits 2 to 9, along with some random cropping. We use a LeNet.

**MNIST results.** Results in Fig. 5 suggest that D-BAT is able to give reliable uncertainty estimates for OOD data-points, even when those samples are away from the boundary decision. This is in sharp contrast with deep-ensemble which only models uncertainty near the boundary decision.

**CIFAR-10 setup.** We train ensembles of 4 models and benchmark three different methods in their ability to identify what they do not know. For this we look at the histograms of the probability of their predicted classes on OOD samples. As training set we use the CIFAR-10 classes  $\{0, 1, 2, 3, 4\}$ . We use the CIFAR-100 (Krizhevsky, 2009) test set as OOD samples to compute the histograms. For D-BAT we use the remaining CIFAR-10 classes,  $\{5, 6, 7, 8, 9\}$ , as  $\mathcal{D}_{\text{ood}}$ , and set  $\alpha$  to 0.2. Histograms are averaged over 5 seeds. The three methods considered are simple deep-ensembles (Lakshminarayanan et al., 2017), MC-Dropout models (Gal & Ghahramani, 2016), and D-BAT ensembles. For the three methods we use a modified ResNet-18 (He et al., 2016) with added dropout to accommodate MC-Dropout, we use a dropout probability of 0.2 for the three methods. For MC-Dropout, we compute uncertainty estimates sampling 20 distributions.

**CIFAR-10 results.** In Fig. 6, we observe for both deep ensembles and MC-Dropout a large amount of predicted probabilities larger than 0.9, which indicate those methods



are overly confident on OOD data. In contrast, most of the predicted probabilities of D-BAT ensembles are smaller than 0.7. The average ensemble accuracies for all those methods are 92% for deep ensembles, 91.2% for D-BAT ensembles, and 90.4% for MC-Dropout.

## 5. Limitations

**Maximum ensemble size.** As D-BAT chooses to view diversity as disagreement of *predicted classes* on the OOD distribution, it is limited by the number of output classes. For a binary classification task, and given an image  $\tilde{x}$  sampled from  $\mathcal{D}_{\text{ood}}$ , if  $h_1(\tilde{x})$  predicts class 0 with high probability, then  $h_2(\tilde{x})$  will try to predict class 1 with high probability to maximize Eq. (AG). A third model would have no space left to disagree on  $\tilde{x}$ . In our experiments, when we increased the ensemble size  $M$  beyond the number of classes, the models  $h_k$  with  $k > M$  predict a flat distribution (max entropy) for samples of  $\mathcal{D}_{\text{ood}}$ .

**Is the simplicity bias gone?** While we showed in § 4.1 that our approach can clearly mitigate shortcut learning, a bad choice of  $\mathcal{D}_{\text{ood}}$  distribution can introduce an additional shortcut. Assuming we train on images of birds and we pick a  $\mathcal{D}_{\text{ood}}$  far away from the training distribution, e.g. pictures of buildings. Then a shortcut to solve the D-BAT objective *without* having to learn to use different features of the input distribution could consist in learning to distinguish OOD images from in-distribution images, e.g. counting the number of corners. Given this OOD detection mechanism, each predictor in the ensemble would be able to rely on the same features (hence no diversity), and still agree on what to predict when confronted to an OOD image, e.g.  $h_1$  only predicts class 1 on OOD,  $h_2$  only predicts class 2 on OOD, etc. In essence, our approach fails to promote diverse representations when differentiating  $\mathcal{D}$  from  $\mathcal{D}_{\text{ood}}$  is easier than learning to utilize diverse features.

## 6. Discussion

Training deep neural networks often results in the models learning to rely on shortcuts present in the training data but absent from the test data. In this work we introduced D-BAT, a novel training method to promote diversity in ensembles of predictors. By encouraging disagreement on OOD data, while agreeing on the training data, we effectively (i) give strong incentives to our predictors to rely on diverse features, (ii) which enhance the transferability of the ensemble and (iii) improve uncertainty estimation and OOD detection. Future directions include improving the selection of samples of the OOD distribution and develop stronger theory.

## References

- Amodei, D., Olah, C., Steinhardt, J., Christiano, P. F., Schulman, J., and Mané, D. Concrete problems in AI safety. *CoRR*, abs/1606.06565, 2016.
- Arjovsky, M., Bottou, L., Gulrajani, I., and Lopez-Paz, D. Invariant risk minimization. *arXiv preprint arXiv:1907.02893*, 2019.
- Arpit, D., Jastrzundzki, S., Ballas, N., Krueger, D., Bengio, E., Kanwal, M. S., Maharaj, T., Fischer, A., Courville, A., Bengio, Y., and Lacoste-Julien, S. A closer look at memorization in deep networks. In *ICML*, pp. 233–242. JMLR, 2017.
- Beery, S., Horn, G. V., and Perona, P. Recognition in terra incognita. In *ECCV (16)*, volume 11220 of *Lecture Notes in Computer Science*, pp. 472–489. Springer, 2018.
- Begoli, E., Bhattacharya, T., and Kusnezov, D. The need for uncertainty quantification in machine-assisted medical decision making. *Nat. Mach. Intell.*, 1(1):20–23, 2019.
- Ben-Tal, A., Ghaoui, L. E., and Nemirovski, A. *Robust Optimization*, volume 28 of *Princeton Series in Applied Mathematics*. Princeton University Press, 2009.
- Bengio, Y., Courville, A., and Vincent, P. Representation learning: A review and new perspectives. *IEEE transactions on pattern analysis and machine intelligence*, 35(8): 1798–1828, 2013.
- Breiman, L. Bagging predictors. *Mach. Learn.*, 24(2): 123–140, 1996.
- Cortes, C. and Mohri, M. Domain adaptation in regression. In *International Conference on Algorithmic Learning Theory*, pp. 308–323. Springer, 2011.
- Cortes, C., Mohri, M., and Medina, A. M. Adaptation based on generalized discrepancy. *The Journal of Machine Learning Research*, 20(1):1–30, 2019.
- Dziugaite, G. K. and Roy, D. M. Computing nonvacuous generalization bounds for deep (stochastic) neural networks with many more parameters than training data. In *Proceedings of the 33rd Annual Conference on Uncertainty in Artificial Intelligence (UAI)*, 2017.
- Gal, Y. and Ghahramani, Z. Dropout as a bayesian approximation: Representing model uncertainty in deep learning. In *ICML*, volume 48 of *JMLR Workshop and Conference Proceedings*, pp. 1050–1059. JMLR.org, 2016.
- Ganin, Y., Ustinova, E., Ajakan, H., Germain, P., Larochelle, H., Laviolette, F., Marchand, M., and Lempitsky, V. Domain-adversarial training of neural networks. *The journal of machine learning research*, 17(1):2096–2030, 2016.

- Geirhos, R., Jacobsen, J., Michaelis, C., Zemel, R. S., Brendel, W., Bethge, M., and Wichmann, F. A. Shortcut learning in deep neural networks. *Nat. Mach. Intell.*, 2 (11):665–673, 2020.
- Gunasekar, S., Lee, J. D., Soudry, D., and Srebro, N. Implicit bias of gradient descent on linear convolutional networks. In *NeurIPS*, pp. 9482–9491, 2018.
- He, K., Zhang, X., Ren, S., and Sun, J. Deep residual learning for image recognition. In *CVPR*, 2016.
- Hernández-Lobato, J. M. and Adams, R. P. Probabilistic backpropagation for scalable learning of bayesian neural networks. In *ICML*, volume 37 of *JMLR Workshop and Conference Proceedings*, pp. 1861–1869. JMLR.org, 2015.
- Ilyas, A., Santurkar, S., Tsipras, D., Engstrom, L., Tran, B., and Madry, A. Adversarial examples are not bugs, they are features. *arXiv preprint arXiv:1905.02175*, 2019.
- Kariyappa, S. and Qureshi, M. K. Improving adversarial robustness of ensembles with diversity training. *CoRR*, abs/1901.09981, 2019.
- Kim, B., Koyejo, O., and Khanna, R. Examples are not enough, learn to criticize! criticism for interpretability. In *NIPS*, pp. 2280–2288, 2016.
- Koyama, M. and Yamaguchi, S. Out-of-distribution generalization with maximal invariant predictor. *arXiv preprint arXiv:2008.01883*, 2020.
- Krizhevsky, A. Learning Multiple Layers of Features from Tiny Images. Master’s thesis, 2009.
- Krueger, D., Caballero, E., Jacobsen, J., Zhang, A., Binas, J., Zhang, D., Priol, R. L., and Courville, A. C. Out-of-distribution generalization via risk extrapolation (rex). In *ICML*, volume 139 of *Proceedings of Machine Learning Research*, pp. 5815–5826. PMLR, 2021.
- Lakshminarayanan, B., Pritzel, A., and Blundell, C. Simple and Scalable Predictive Uncertainty Estimation Using Deep Ensembles. In *Proceedings of the 31st International Conference on Neural Information Processing Systems*, pp. 6405–6416, Red Hook, NY, USA, 2017. Curran Associates Inc.
- Lecun, Y. and Cortes, C. The MNIST database of handwritten digits. 1998. URL <http://yann.lecun.com/exdb/mnist/>.
- Lecun, Y., Bottou, L., Bengio, Y., and Haffner, P. Gradient-based learning applied to document recognition. In *Proceedings of the IEEE*, pp. 2278–2324, 1998.
- Lin, T., Maire, M., Belongie, S. J., Hays, J., Perona, P., Ramanan, D., Dollár, P., and Zitnick, C. L. Microsoft COCO: common objects in context. In *ECCV (5)*, volume 8693 of *Lecture Notes in Computer Science*, pp. 740–755. Springer, 2014.
- Liu, Y., Pagliardini, M., Chavdarova, T., and Stich, S. U. The peril of popular deep learning uncertainty estimation methods. 2021.
- Long, M., Cao, Z., Wang, J., and Jordan, M. I. Conditional adversarial domain adaptation. *arXiv preprint arXiv:1705.10667*, 2017.
- Loshchilov, I. and Hutter, F. Decoupled weight decay regularization. In *ICLR (Poster)*. OpenReview.net, 2019.
- Mansour, Y., Mohri, M., and Rostamizadeh, A. Domain adaptation: Learning bounds and algorithms. *arXiv preprint arXiv:0902.3430*, 2009.
- McCoy, T., Pavlick, E., and Linzen, T. Right for the wrong reasons: Diagnosing syntactic heuristics in natural language inference. In *ACL (1)*, pp. 3428–3448. Association for Computational Linguistics, 2019.
- Oakden-Rayner, L., Dunnmon, J., Carneiro, G., and Ré, C. Hidden stratification causes clinically meaningful failures in machine learning for medical imaging. In *CHIL*, pp. 151–159. ACM, 2020.
- Piosenka, G. *325 Bird Species Dataset*. Kaggle, 2020.
- Rahimian, H. and Mehrotra, S. Distributionally robust optimization: A review. *arXiv preprint arXiv:1908.05659*, 2019.
- Ramé, A. and Cord, M. DICE: diversity in deep ensembles via conditional redundancy adversarial estimation. In *ICLR*. OpenReview.net, 2021.
- Rasmussen, C. E. and Williams, C. K. I. *Gaussian Processes for Machine Learning (Adaptive Computation and Machine Learning)*. The MIT Press, 2005.
- Ross, A. S., Pan, W., Celi, L. A., and Doshi-Velez, F. Ensembles of locally independent prediction models. In *AAAI*, pp. 5527–5536. AAAI Press, 2020.
- Sagawa, S., Koh, P. W., Hashimoto, T. B., and Liang, P. Distributionally robust neural networks. In *ICLR*. OpenReview.net, 2020.
- Shah, H., Tamuly, K., Raghunathan, A., Jain, P., and Netrapalli, P. The pitfalls of simplicity bias in neural networks. In *Advances in Neural Information Processing Systems*, volume 33, 2020.

- Sinha, S., Bharadhwaj, H., Goyal, A., Larochelle, H., Garg, A., and Shkurti, F. DIBS: diversity inducing information bottleneck in model ensembles. In *AAAI*, pp. 9666–9674. AAAI Press, 2021.
- Stickland, A. C. and Murray, I. Diverse ensembles improve calibration. *CoRR*, abs/2007.04206, 2020.
- Sun, B., Feng, J., and Saenko, K. Return of frustratingly easy domain adaptation. In *AAAI*, pp. 2058–2065. AAAI Press, 2016.
- Szegedy, C., Zaremba, W., Sutskever, I., Bruna, J., Erhan, D., Goodfellow, I. J., and Fergus, R. Intriguing properties of neural networks. In *ICLR (Poster)*, 2014.
- Teney, D., Abbasnejad, E., Lucey, S., and van den Hengel, A. Evading the simplicity bias: Training a diverse set of models discovers solutions with superior OOD generalization. *CoRR*, abs/2105.05612, 2021.
- Tishby, N., Pereira, F. C., and Bialek, W. The information bottleneck method, 2000.
- Ueda, N. and Nakano, R. Generalization error of ensemble estimators. In *ICNN*, pp. 90–95. IEEE, 1996.
- van Amersfoort, J., Smith, L., Teh, Y. W., and Gal, Y. Uncertainty estimation using a single deep deterministic neural network. In *ICML*, volume 119 of *Proceedings of Machine Learning Research*, pp. 9690–9700. PMLR, 2020.
- Welinder, P., Branson, S., Mita, T., Wah, C., Schroff, F., Belongie, S., and Perona, P. Caltech-UCSD Birds 200. Technical Report CNS-TR-2010-001, California Institute of Technology, 2010.
- Xiao, H., Rasul, K., and Vollgraf, R. Fashion-MNIST: a novel image dataset for benchmarking machine learning algorithms. *arXiv:1708.07747*, 2017.
- Zhou, Z.-H. *Ensemble Methods: Foundations and Algorithms*. Chapman & Hall/CRC, 2012. ISBN 1439830037.

## A. Source code

Link to the source code to reproduce our experiments: <https://github.com/mpagli/Agree-to-Disagree>

## B. Proof of Thm.3.1

We redefine here the setup for clarity:

- Given a joint source distribution  $\mathcal{D}$  of triplets of random variables  $(C, S, Y)$  taking values in  $\{0, 1\}^3$ .
- Assuming  $\mathcal{D}$  has the following pmf:  $\mathbb{P}_{\mathcal{D}}(C = c, S = s, Y = y) = 1/2$  if  $c = s = y$ , and 0 otherwise.
- Assuming a first model learnt the posterior distribution  $\hat{\mathbb{P}}_1(Y = 1 | C = c, S = s) = c$ .
- Given a distribution  $\mathcal{D}_{\text{ood}}$  uniform over  $\{0, 1\}^3$  outside of the support of  $\mathcal{D}$ .

From there, training a second model  $h_2$  following the D-BAT objective would mean minimizing the agreement on  $\mathcal{D}_{\text{ood}}$ :

$$\min_{(c,s) \sim \mathcal{D}_{\text{ood}}} \mathbb{E} \left[ -\log(\hat{\mathbb{P}}_1(Y = 1|c, s)\hat{\mathbb{P}}_2(Y = 0|c, s) + \hat{\mathbb{P}}_1(Y = 0|c, s)\hat{\mathbb{P}}_2(Y = 1|c, s)) \right] \quad (1)$$

While at the same time agreeing on the source distribution  $\mathcal{D}$ :

$$\mathbb{P}_{(c,s) \sim \mathcal{D}} \left( \hat{\mathbb{P}}_1(Y|c, s) = \hat{\mathbb{P}}_2(Y|c, s) \right) = 1$$

The expectation in eq.1 becomes:

$$(1) = \frac{1}{2} \left( -\log(\hat{\mathbb{P}}_2(Y = 0|C = 1, S = 0)) - \log(\hat{\mathbb{P}}_2(Y = 1|C = 0, S = 1)) \right)$$

Which is minimized for  $\hat{\mathbb{P}}_2(Y = 1|C = 0, S = 1) = \hat{\mathbb{P}}_2(Y = 0|C = 1, S = 0) = 1$ .

Which means the posterior of the second model, according to our disagreement constrain, will be:

$$\hat{\mathbb{P}}_2(Y = 1 | C = c, S = s) = s$$

## C. Omitted details on experiments

### C.1. Architecture used in § 4.1

In the experiments on mitigating shortcut learning, we used differnt versions of LeNet ([Lecun et al., 1998](#)):

- For the C-MNIST dataset, we used a standard LeNet, with 3 input channels instead of 1.
- For the MM-Dominoes and MF-Dominoes datasets, we increase the input dimension of the first fully-connected layer to 960.
- For the MC-Dominoes dataset, we use 3 input channels, increase the number of output channels of the first convolution to 32, and of the second one to 56. We modify the fully-connected layers to be  $2016 \rightarrow 512 \rightarrow 256 \rightarrow c$  with  $c$  the number of classes.

For further details on the implementation, we invite the reader to check the source code, see § A.



### C.2. Implementation details for Fig.1

Instead of relying on an external OOD distribution set, it is also possible to find, given some datapoint  $\mathbf{x}$ , a perturbation  $\delta^*$  through directly minimizing the agreement in some neighborhood of  $\mathbf{x}$  (i.e. for  $\|\delta^*\| \leq \epsilon$ ):

$$\delta^* \in \arg \min_{\delta \text{ s.t. } \|\delta\| < \epsilon} -\log (p_{h_1,(\mathbf{x}+\delta)}^{(0)} \cdot p_{h_2,(\mathbf{x}+\delta)}^{(1)} + p_{h_1,(\mathbf{x}+\delta)}^{(1)} \cdot p_{h_2,(\mathbf{x}+\delta)}^{(0)})$$

Which can be solved using several projected gradient descent steps as it done typically in the adversarial training literature. While this approach is working for the 2D example, it is not working however for complex high-dimensional input spaces combined with deep networks as those are notorious for their sensitivity to very small  $l_p$ -bounded perturbations, and it would most of the time be easy to find a bounded perturbation maximizing the disagreement.

### C.3. Implementation details for Kaggle-Bird experiments

We resize images to a resolution of  $128 \times 128$ , and use a ResNet-50 (He et al., 2016) as model. We train for 60 epochs with a triangular learning rate scheduler with  $lr_{\max} = 0.2$  and SGD as optimizer.

## D. OOD distribution samples for § 4.1

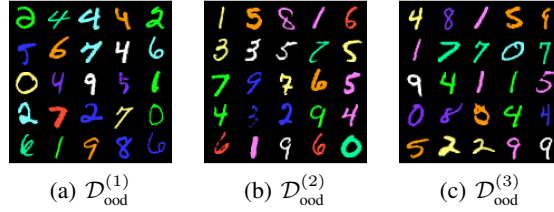


Figure 7. OOD distributions used for the C-MNIST experiments

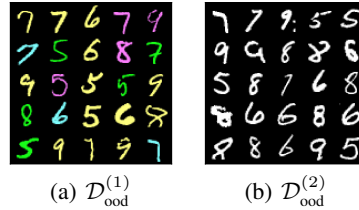


Figure 8. OOD distributions used for the C-MNIST—half experiments

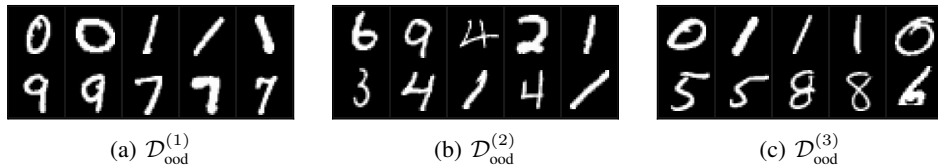


Figure 9. OOD distributions used for the MM-Dominoes experiments

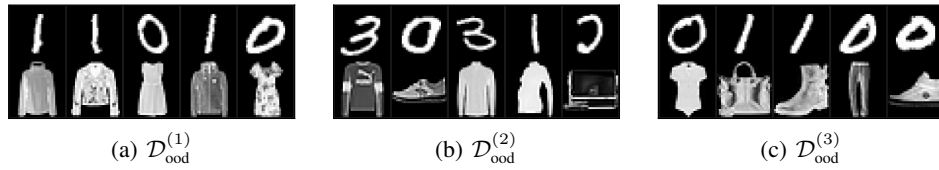


Figure 10. OOD distributions used for the MF-Dominoes experiments

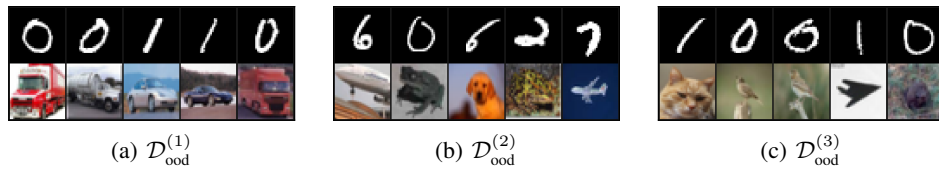


Figure 11. OOD distributions used for the MC-Dominoes experiments